

Study of electron traps in *n*-GaAs grown by molecular beam epitaxy

D. V. Lang, A. Y. Cho, A. C. Gossard, M. Illegems, and W. Wiegmann

Bell Laboratories, Murray Hill, New Jersey 07974

(Received 17 December 1975)

Electron trapping centers in *n*-GaAs grown by molecular beam epitaxy (MBE) have been studied by deep-level transient capacitance spectroscopy (DLTS). At least nine different electron traps are observed with energies ranging from 0.08 to 0.85 eV from the conduction band. Total electron trap concentrations in various samples range from the low 10^{14} cm^{-3} range to the mid 10^{12} cm^{-3} range. Studies of samples from various growth systems indicate that these traps are most likely due to chemical impurities. A comparison is made with electron traps in *n*-GaAs grown by vapor- and liquid-phase epitaxy as well as with the electron traps introduced into *n*-GaAs by 1-MeV electron irradiation.

PACS numbers: 71.55.Fr, 72.20.Kw, 61.70.Wp

I. INTRODUCTION

Molecular beam epitaxy (MBE) has proven to be an extremely useful technique for growing thin epitaxial films of GaAs with high uniformity. This, coupled with the ability to precisely tailor doping profiles, makes possible the fabrication of MBE GaAs majority-carrier devices such as varactor diodes,¹ high-frequency FET's,² IMPATT diodes,³ and mixer diodes.⁴ These majority-carrier *n*-type devices are sensitive to the presence of electron traps in the material. Asai *et al.*⁵ have shown that an impurity-related electron trap at approximately 0.4 eV from the conduction band adversely affects the microwave-frequency characteristics of *n*-GaAs Schottky-barrier gate FET's fabricated by vapor-phase epitaxy (VPE). Mircea and Mitanneau⁶ have recently used the technique of deep-level transient spectroscopy (DLTS)⁷ to record the spectra of electron traps in VPE *n*-GaAs and find four different traps in various samples with activation energies to the conduction band of 0.83, 0.58, 0.42, and 0.18 eV, respectively. They find no electron traps in GaAs grown by liquid-phase epitaxy (LPE), however. Hasegawa and Majerfeld⁸ recently studied VPE and LPE GaAs by the capacitance transient technique and observed the 0.83-eV electron trap in VPE *n*-GaAs and no electron traps in LPE *n*-GaAs.

We report here for the first time a systematic study of electron traps in MBE *n*-GaAs grown in six different systems with three different dopants (Si, Sn, and Ge) under both As- and Ga-rich growth conditions. The electron traps observed in MBE *n*-GaAs are compared with those in VPE, LPE, and electron-irradiated *n*-GaAs. The electron traps in LPE *n*-GaAs are observed here for the first time. The deep-level spectra were recorded by the DLTS technique.⁷

In Sec. II we discuss the measurement technique and crystal growth. The DLTS spectra are presented in Sec. III. Section IV is a comparison of the MBE *n*-GaAs electron traps with those observed in VPE *n*-GaAs, LPE *n*-GaAs, and 1-MeV electron-irradiated LPE *n*-GaAs. The results and conclusions are summarized in Sec. V.

II. EXPERIMENTAL TECHNIQUE

A. Crystal growth

The basic MBE growth system has been discussed by Cho.⁹ For this study we have looked at electron traps in single *n*-type MBE layers, 2–4 μ in thickness, grown on both Cr-doped semi-insulating and Si- or Te-doped *n*-type substrates. Three different *n*-type dopants were studied (Si, Sn, and Ge). The samples were grown in six different MBE growth systems. Systems 1, 2, and 3 used the "first-generation" MBE growth arrangement discussed in Ref. 9. Systems 4, 5, and 6 are more recent with more careful attention given to the reduction of spurious impurities.¹

Typical substrate preparation techniques for systems 1, 3, 4, and 6 used a Br_2 -methanol etch⁹ followed by a rinsing in deionized water and drying with nitrogen gas. Sample preparation for systems 2 and 5 used the same etch with an ultrasonic methanol rinse followed by a condensed methanol vapor flushing and air drying. Both preparation techniques resulted in a thin oxide layer on the sample. Subsequent removal of this oxide in the MBE ultrahigh vacuum system was accomplished by heating to above 530 °C and provided a nearly atomically clean substrate.¹

All but one of the samples were grown under As-rich conditions as evidenced by the characteristic As stabilized surface reconstruction pattern observed *in situ* during growth by high-energy electron diffraction (HEED).¹⁰ The one exception to As stabilized growth was a sample grown with an As-to-Ga ratio and temperature which resulted in a different surface reconstruction typical of more nearly Ga stabilized growth.¹⁰ The predominant source of As was α As, except system 1 which used polycrystalline GaAs. Typical growth temperatures ranged from 540 to 610 °C at growth rates of 0.5–2 $\mu\text{m/h}$.

The residual gas in an ultrahigh vacuum system usually contains H_2 , CO, and H_2O . The reduction of these background gases is accomplished by gettering and condensation using Ti sublimation and liquid-nitrogen-cooled panels. The CO and H_2O background during deposition is on the order of 10^{-9} Torr for systems 4, 5, and 6.

B. Schottky-barrier fabrication

Schottky barriers were fabricated on the MBE layers by evaporating a thin layer of Cr ($\sim 100 \text{ \AA}$) followed by a layer of Au through a mask with 10–20-mil-diam circular openings. Ohmic contacts were made to the epitaxial layer by arc melting a Sn-doped Au wire into the layer. The samples were then mounted on TO-18 headers with silver-filled epoxy and contacted by conventional thermocompression bonding. Carrier concentrations were measured on a C - V feedback profiler.¹¹

C. DLTS

The spectra of electron traps in these Schottky-barrier samples were obtained by the DLTS technique as discussed in Ref. 7. An electron trap is defined⁷ to be any deep level for which the electron thermal emission rate is much larger than the hole thermal emission rate. In general, such a level tends to be in the upper-half of the gap. Electron traps defined in this manner may be readily observed as negative majority-carrier-type DLTS signals by using Schottky barriers on n -type GaAs. Hole traps, on the other hand, are not detectable in n -type Schottky-barrier samples by the normal DLTS technique. Future work with pn junctions is planned to study the hole traps in MBE GaAs. In this work we are

studying single n -type epitaxial layers with Schottky barriers and thus will discuss only electron trap spectra.

The DLTS spectra were recorded with a standardized rate window of 51 sec^{-1} . The double-boxcar 5-msec gates were set at 4.5 and 37.8 msec to obtain this rate window and suppress 60-Hz interference. The saturating majority-carrier pulse in all cases was $10 \text{ }\mu\text{sec}$ in duration with an amplitude equal to the quiescent reverse bias (typically -2 to -6 V). In several samples the trap concentration was carefully measured by the $\delta(\Delta C/C)$ -vs- δV technique discussed in Ref. 7. This concentration was then used to calibrate the DLTS peak height for $V_M = -V_B$, where V_M is the majority-carrier pulse height and V_B is the reverse bias on the barrier. Under these conditions an empirical relationship given by

$$N_T = 3[\Delta C(0)/C](N_D - N_A) \quad (1)$$

was observed to hold in nearly all cases. In Eq. (1), N_T is the trap concentration, $N_D - N_A$ is the net shallow donor concentration, $\Delta C(0)$ is the DLTS peak height in capacitance units corrected to the $t=0$ value using the exponential approximation,⁷ and C is the barrier capacitance at the reverse bias being used. Note that Eq. (1) gives 1.5 times larger trap concentrations than the expression obtained from assuming all traps in the

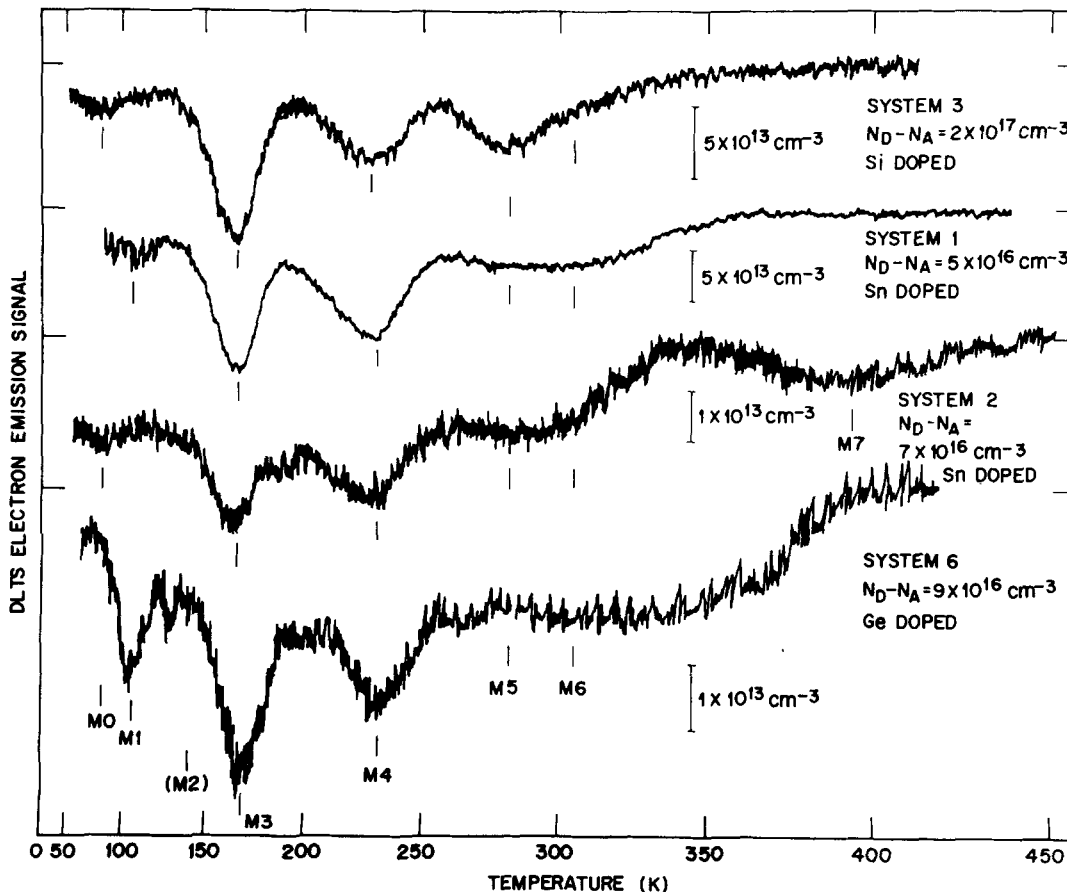


FIG. 1. DLTS spectra of electron traps (negative peaks) in MBE n -GaAs grown in four different systems with three different dopants (Si, Sn, and Ge) under As-rich growth conditions. The rate window is 51 sec^{-1} . The trap concentration scale is indicated for each trace. Note the similarity in spectra.

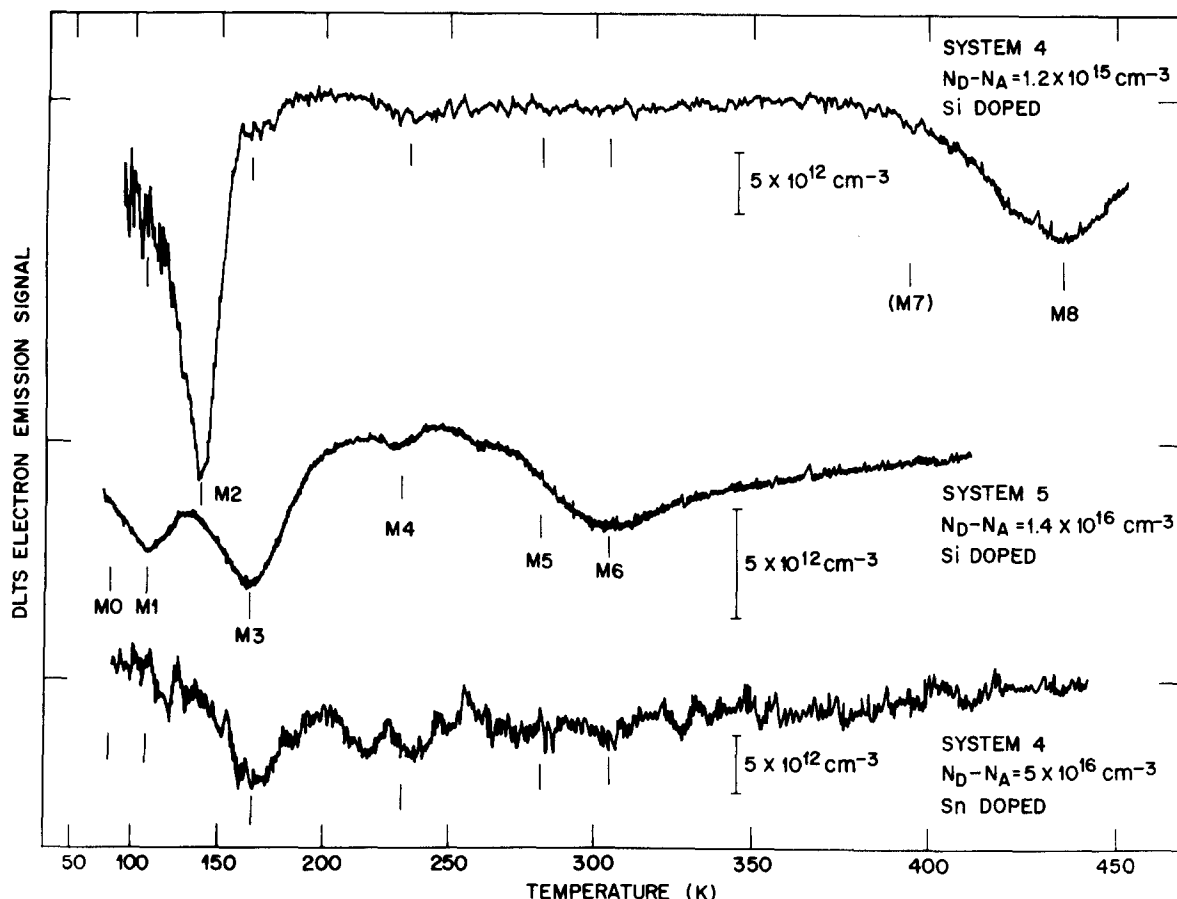


FIG. 2. DLTS spectra of electron traps in MBE n -GaAs showing two As-rich samples with lowest trap concentrations (lower two traces) and a Ga-rich sample (upper trace). The rate window is 51 sec^{-1} . The trap concentration scale is indicated for each trace.

depletion region have been filled [see Eq. (3), Ref. 7]. Thus, apparently only about two-thirds of the traps in the depletion region are filled by the majority-carrier pulse used here.

III. EXPERIMENTAL RESULTS

A. Electron trap spectra

The DLTS spectra of MBE n -GaAs layers grown in six different systems are shown in Figs. 1 and 2. Note in Fig. 1 the similar DLTS spectra obtained in layers grown in four different systems (1, 2, 3, and 6) using three different dopants (Si, Sn, and Ge) under As-rich growth conditions. The observed electron emission signals from the traps (negative peaks) are marked in the figures and labeled M0, M1, ..., M8. Not all samples show all of these deep levels and some levels are not resolved in some samples. As shown in Fig. 1, the dominant trap levels in all As-rich layers are M3 and M4 with concentrations varying from a maximum of $1.6 \times 10^{14} \text{ cm}^{-3}$ for M3 in system 1 to the mid 10^{12} cm^{-3} range in systems 4 and 5 (Fig. 2). Note the unresolved smear of several traps in the region of M5 and M6. The M5 level is resolved only in the upper trace in Fig. 1, while M6 is seen clearly only in the middle trace of Fig. 2. The lower trace in Fig. 1 suggests that there may be other unresolved traps between M6 and M7. The upper trace in Fig. 2 shows the strikingly different

spectrum obtained in a sample grown under Ga-rich conditions.

The thermal emission rates for the most common traps in As-rich samples (M0, M1, M3, and M4) are shown as a function of inverse temperature in Fig. 3. The slope of this data gives an activation energy which we will denote ΔE_{meas} , given in Fig. 3. This value includes the T^2 dependence of the exponential prefactor and can be easily corrected by subtracting $2kT$, where T is the average temperature of the range of measurement. The activation energy with this T^2 correction, ΔE , is given in Fig. 3 in parenthesis. This data is summarized in Table I along with the exponential prefactors for traps M0, M1, M3, and M4 and approximate energy levels for the other five less common or difficult to resolve traps shown in Figs. 1 and 2.

The data in Table I can be understood by recalling the detailed balance relationship

$$e_{\text{th}} = \langle \sigma_v \rangle N_c / g \exp(\Delta E / kT), \quad (2)$$

where e_{th} is the thermal emission rate of a trapped electron, $\langle v \rangle$ is the average thermal velocity of an electron, N_c is the density of states in the conduction band, g is the degeneracy factor, k is Boltzmann's constant, ΔE is the T^2 -corrected apparent activation energy (which includes the barrier to thermal capture, E_∞),

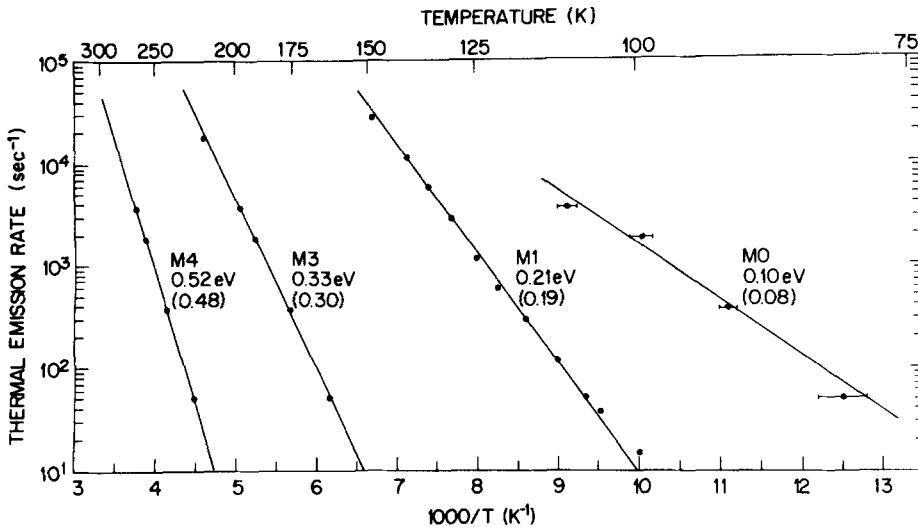


FIG. 3. Thermal emission rates vs inverse temperature for electron traps M0, M1, M3, and M4. The activation energies shown by each curve are ΔE_{meas} and, in parenthesis, $\Delta E = \Delta E_{\text{meas}} - 2kT$.

and σ_{∞} is the exponential prefactor of the electron-capture cross section^{12,13}

$$\sigma_n = \sigma_{\infty} \exp(-E_{\infty}/kT). \quad (3)$$

The values of the prefactor in Eq. (2) are given in Table I for those traps measured in Fig. 3. The apparent activation energy ΔE can be given approximately for the other less common traps by assuming a typical prefactor value and using the rate window setting and DLTS peak position in Eq. (2). We give only an approximate energy for these five levels since they only occur in a few samples (M2 and M8) or are broad low-concentration peaks which are often difficult to resolve well enough to obtain accurate data such as in Fig. 3. In Table I at a rate window of 51 sec⁻¹ and assuming a prefactor of 10¹² sec⁻¹ we find $\Delta E \approx 23.7kT$, where T is the DLTS peak position at this rate window. Since ΔE depends only logarithmically on the prefactor, this ΔE value is accurate to approximately $\pm 10\%$.

B. Electron-capture cross sections

An attempt was made to measure directly the electron-capture cross sections of traps M1, M3, and M4 by the methods discussed in Refs. 7, 12, and 13, but the cross sections were too large to measure in these relatively heavily doped samples. We observed complete filling of the traps with a majority-carrier pulse of 50 nsec in duration. The electron capture rate c is related to the electron-capture cross section σ_n by

$$c = \sigma_n \langle v \rangle n, \quad (4)$$

where $\langle v \rangle$ is the average thermal velocity and n is the concentration of free electrons. Using $c > (20 \text{ nsec})^{-1}$, $\langle v \rangle = 2.8 \times 10^7 \text{ cm/sec}$ and $n = 7 \times 10^{18} \text{ cm}^{-3}$, we find

$$\sigma_n > 2.6 \times 10^{-17} \text{ cm}^2. \quad (5)$$

An indirect measure of σ_{∞} may be obtained from the thermal-emission-rate prefactor given in Table I [see Eqs. (2) and (3)]. At $T = 150 \text{ K}$ with $N_c \langle v \rangle = 5 \times 10^{24} \text{ cm}^{-2} \text{ sec}^{-1}$ and $g = 1$, the σ_{∞} values are 1.2×10^{-14} , 2.6×10^{-14} , and $7.9 \times 10^{-13} \text{ cm}^2$ for traps M1, M3, and M4, respectively. We should note, however, that the values of σ_{∞} obtained in this way from the prefactor are typically about an order of magnitude larger than the actual σ_{∞}

value obtained by direct measurement.^{12,13} It can be shown from the data in Ref. 12 that this approximate order-of-magnitude discrepancy holds for all GaAs traps for which σ_{∞} has been measured directly, i.e., hole traps A, B, Cu (0.44 eV), and Fe as well as electron traps E3 and O.¹² Such a discrepancy in the case of the O trap has also been pointed out by Mircea and Miteneau.⁶ The reason for such a discrepancy is unclear but may be related to the fact that the exponential prefactor is measured in the presence of a rather strong junction electric field whereas the direct cross-section measurements are made in neutral material at zero electric field. If the σ_{∞} values calculated above for M1, M3, and M4 are reduced by approximately this factor of 10, they fall reasonably close to the range of σ_{∞} values predicted and observed by Lang and Henry to correspond to nonradiative capture by multiphonon emission.¹³

These three dominant MBE levels thus appear to be very effective electron traps with capture times which can be estimated from Eq. (4) to be on the order of 500 psec at 300 K for $\sigma_n = 1 \times 10^{-15} \text{ cm}^2$, $\langle v \rangle = 4 \times 10^7 \text{ cm/sec}$,

TABLE I. Measured properties of nine electron traps in MBE n -GaAs. ΔE_{meas} is the slope of the log of the electron thermal emission rate vs inverse temperature. ΔE is the emission activation energy corrected for the T^2 dependence of the prefactor. $\sigma_{\infty} \langle v \rangle N_c$ is the prefactor of the thermal emission rate at the temperature of measurement. The ΔE values in the right-hand column are approximations derived from the DLTS peak position.

Electron trap	MBE electron trap parameters			
	ΔE_{meas} (eV)	$\Delta E = \Delta E_{\text{meas}} - 2kT$ (eV)	$\sigma_{\infty} \langle v \rangle N_c / g$ (sec ⁻¹)	$\Delta E \approx 23.7kT \pm 10\%$ (eV)
M0	0.10	0.08	1.5×10^7	...
M1	0.21	0.19	6.1×10^{10}	...
M2	0.29
M3	0.33	0.30	1.3×10^{11}	...
M4	0.52	0.48	4.0×10^{12}	...
M5	0.58
M6	0.62
M7	0.81
M8	0.85

and $n = 5 \times 10^{16} \text{ cm}^{-3}$. In addition, the extrapolated thermal emission times of traps M1, M3, and M4 at 300 K can be obtained from Eq. (2) and Table I as 6 nsec, 0.4 μsec , and 20 μsec , respectively. A trap such as M1 which can capture and reemit electrons on the scale of nanoseconds at 300 K could cause frequency response and noise problems in majority-carrier devices operating in the GHz range. This is not likely, however, for the very low trap concentrations seen in the best samples studied here.

We should note also that these traps could not strongly affect the minority-carrier lifetime in these samples because of their low concentration. Even if both the hole and electron-capture cross sections were large ($\sigma \sim 10^{-14} \text{ cm}^2$) and the deep level was thus a good recombination center, the contribution of such traps at the 10^{13} cm^{-3} concentration level to the minority-carrier lifetime would be several hundred nsec, which is negligible. Thus the deep-level spectrum of the samples shown in Fig. 2 would not limit the operation of minority-carrier injection devices such as MBE GaAs-Al_xGa_{1-x}As double-heterostructure lasers.^{14,15} Indeed, MBE *n*-type layers doped with Sn and Si have even better photoluminescence efficiency than comparable layers grown by LPE.¹⁵ This shows that the total concentration of effective bulk recombination centers ($\sigma \sim 10^{-14} \text{ cm}^2$) in these layers is certainly less than a few times 10^{13} cm^{-3} .

C. Trap concentrations in different MBE systems

We note on the one hand that the main spectral features in Fig. 1 are quite independent of growth system for the four systems (1, 2, 3, and 6) and three dopants (Si, Sn, and Ge) shown. This indicates that the source of the defects which create these traps under As-rich growth conditions is common to most MBE growth systems. The question naturally arises as to whether these electron traps are due to chemical impurities or to native lattice defects, such as vacancies, interstitials, or simple complexes. To answer this point we note that there is a definite trend of reduced trap concentrations between systems 1, 2, 3, and 6 on the one hand (Fig. 1) and systems 4 and 5 on the other (Fig. 2, lower 2 traces) with improvements of nearly a factor of 30 from the worst to best case. It is significant that this reduction in trap concentrations can be directly correlated with efforts to reduce sources of spurious contamination in systems 4 and 5. Hence, it may be concluded that the electron traps observed here are related to chemical impurities and are not simple lattice defects, since the concentration of native defects should depend primarily on the growth parameters such as temperature, stoichiometry, and growth rate, and not strongly on low-level contaminants.

Stoichiometry differences are important, however, in the upper trace of Fig. 2. This sample, grown in system 4 and lightly doped with Si, is the only example shown which was grown near Ga-rich conditions.¹⁰ All other samples shown in Figs. 1 and 2 were grown under the more typical As-rich conditions. There is a marked difference in DLTS spectra between Ga- and As-rich growth conditions. As seen in the upper trace of Fig.

2, traps M2 and M8 are the main features of a Ga-rich sample but are not present in *any* of the As-rich samples. Traps M3 and M4, which are dominant in the As-rich samples, are just barely visible at about $1 \times 10^{12} \text{ cm}^{-3}$ in the Ga-rich sample. To show that these rather striking spectral differences are, in fact, due to growth stoichiometry we note that the upper and lower traces in Fig. 2 were both grown in system 4 at 580 °C with the upper trace Ga rich and the lower As rich. Furthermore, as pointed out above, the main features of the As-rich spectra are quite reproducible in six different MBE growth systems with three different dopants (Si, Sn, and Ge) and a variety of growth temperature and growth rates.

The strong dependence of the spectra on growth stoichiometry might lead one to suspect that the systematic dependence of the As-rich spectra on system cleanliness could possibly be due instead to systematic variations in the As-to-Ga ratio while still in the over-all As-rich condition. The As-rich growth condition, as evidenced by the characteristic As stabilized surface reconstruction observed by HEED, is stable over a rather large range of As-to-Ga ratios.¹⁰ Thus, As-rich growth conditions might be expected to be quite similar in the various systems without precise equality in the As-to-Ga ratios. Changes in the As/Ga ratio within the As stabilized regime might have a small effect on trap concentrations, but most likely it would be less than the change in concentration between As- and Ga-rich growth. We find, however, that the differences in trap concentration between the various As-rich samples (up to a factor of about 30 for traps M3 and M4) is considerably larger than the suppression (by a factor of only about 5) in traps M3 and M4 due to Ga-rich growth vs As-rich growth for the same system (number 4) as shown in Fig. 2. In fact, the spectrum of system 1 (Fig. 1) corresponded to slightly less As (with constant Ga flux) than the spectrum of system 4 (Fig. 2) even though the M3 and M4 trap concentrations in system 1 were over 20 times larger than in system 4. Finally, as pointed out above, the traps characteristic of Ga-rich growth (M2 and M8) are not detectable in *any* of the As-rich samples. Thus, it is unlikely that the systematic variations among the As stabilized samples is due to variations in As/Ga stoichiometry, but rather due to the systematic suppression of chemical contaminants by various means in the more recent systems.

It is of interest to point out that other properties of MBE GaAs have also been observed to depend strongly on growth stoichiometry. First, Ge has been observed to act as a donor under As stabilized growth conditions but as an acceptor under Ga stabilized conditions.¹⁶ Striking differences have also been observed in the photoluminescence spectra of undoped MBE layers grown under these two conditions.^{17,18}

The large stoichiometric difference in DLTS spectra leads one to suspect that the defects involved are in some way related to Ga or As vacancies, either directly as native defects or complexes, or indirectly by the vacancies influencing the solubility of impurities. As we will show in Sec. IV, however, none of the MBE electron traps occur in 1-MeV electron-

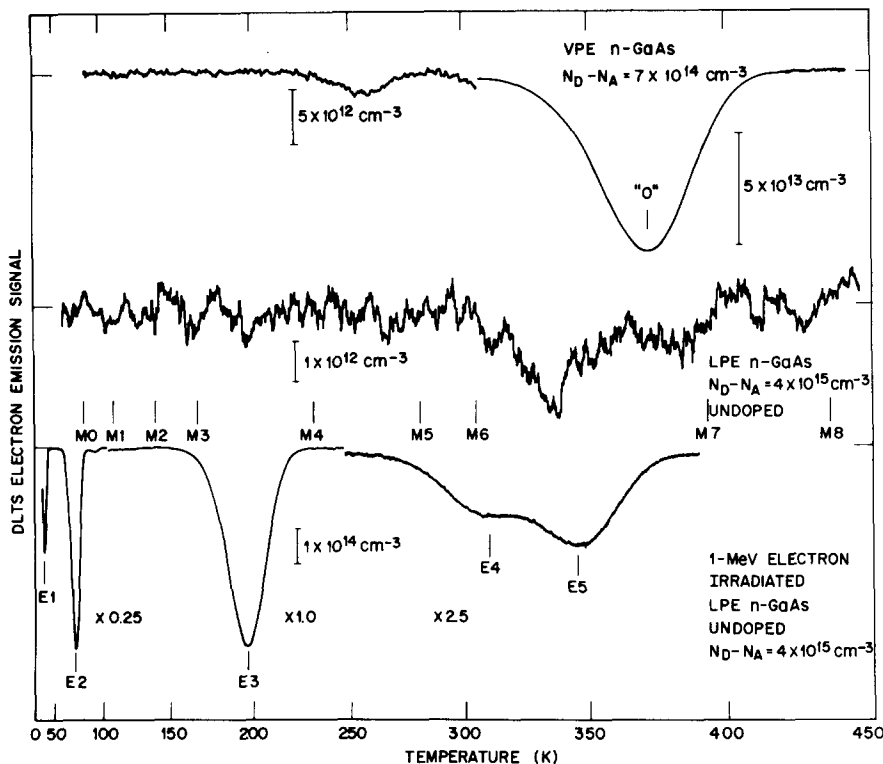


FIG. 4. DLTS spectra of electron traps in VPE and LPE n -GaAs (upper two traces) and in 1-MeV electron-irradiated n -GaAs (lower trace). The positions of the MBE traps M0, M1, ..., M8 are noted above the lower trace. The rate window is 51 sec^{-1} . The trap concentration scale is indicated for each trace.

irradiated n -GaAs. Hence, we may conclude that the MBE traps are not simple native defects but are more likely chemical impurities and/or complexes of chemical impurities with native defects. The traps in As-rich MBE n -GaAs appear to be related to chemical impurities since their concentration depends on the cleanliness of the growth system. The M2 and M8 Ga-rich traps may also be due to some impurity which has a greater solubility in Ga-rich samples than in As-rich samples. However, the evidence for the chemical nature of these traps is not as strong as for the case of the As-rich samples.

IV. COMPARISON WITH OTHER GROWTH TECHNIQUES

In this section we will compare the electron traps observed in MBE n -GaAs with those observed in high-quality VPE and LPE n -GaAs as well as with the native defect electron traps controllably introduced into LPE n -GaAs by 1-MeV electron irradiation. Figure 4 shows the DLTS spectra of these three types of samples taken with the same rate window as Figs. 1 and 2 (51 sec^{-1}). The locations of the MBE traps M0, M1, ..., M8 is denoted in Fig. 4 just above the lower trace. Note that, with the possible exception of M6, none of the MBE traps are the same as traps in the other three types of material. A comparison of the type shown in Fig. 4 is perhaps the best way to relate traps observed in different samples. The DLTS peak position at a fixed rate window is more specific of a particular deep level than is the energy-level value alone since the DLTS peak position contains information on the prefactor as well as the activation energy. It is especially misleading to compare thermal activation energies with energies determined

optically by luminescence, absorption, or photo-capacitance. Such a comparison can give a great deal of information about the lattice relaxation associated with a particular defect, but because of this relaxation the energies determined by the two types of spectroscopy (optical vs thermal) can be somewhat different.

The two electron traps in the VPE n -GaAs (upper trace in Fig. 4) are quite typical of high-quality epitaxial material. They are the same levels reported by Mircea and Mitonneau (MM)⁶ which they labeled A and B. We have labeled the larger VPE peak at about 370 °C as O since it has the same (corrected) energy as the deep level in O-doped semi-insulating GaAs ($E_c - 0.75$ eV).¹² This corresponds to peak A of MM and as they and others¹⁹ point out it is presented in *all* VPE GaAs. The shallower electron traps observed by MM (B, C, and F) are sometimes not seen, indicating that chemical impurities may be responsible just as for the electron traps in MBE GaAs.

The n -type LPE GaAs layer shown in the middle trace of Fig. 4 shows only two very weak signals in the low 10^{12} cm^{-3} range. These may correspond to level O in VPE GaAs and level E5 in electron irradiated GaAs. This is the first time that *any* electron traps have been observed in as-grown undoped LPE n -GaAs. (Two hole traps, A and B, are commonly observed, however).¹² In any event, it is clear that the MBE electron traps are not the same as those in LPE GaAs.

Growth stoichiometry no doubt plays a role in the differences between the trap spectra of VPE and LPE GaAs just as for the case of Ga- and As-rich MBE

GaAs. LPE GaAs corresponds to the extreme limit of Ga-rich growth conditions, whereas VPE growth corresponds to more As-rich conditions. Thus, even though the shallow electron traps in VPE GaAs appear to be related to chemical impurities, it is noteworthy that growth stoichiometry plays an important role in their incorporation since these traps are never seen in LPE GaAs.

Finally, we compare the MBE electron traps with those introduced into LPE *n*-GaAs by 1-MeV electron irradiation at room temperature.²⁰ These radiation traps are most likely due to native defects such as vacancies, interstitials, and simple complexes. Note that only M6 and E4 appear to be similar. This may not mean that they are the same, however, since the M5-M6 region of the MBE spectrum is difficult to resolve and apparently due to several traps, perhaps more than two. It is significant that none of the other MBE electron traps is even close to the radiation defects. This agrees with our earlier conclusion based on comparisons of different growth systems that the MBE traps are most likely due to chemical contaminants (either as isolated species or complexed with native defects) and not simple native defects.

V. CONCLUSIONS

We have used the DLTS capacitance spectroscopy technique to study electron traps in *n*-GaAs grown by molecular beam epitaxy (MBE). We find nine electron traps ranging in depth from 0.08 to 0.85 eV from the conduction band. Different spectra are observed corresponding to Ga- and As-rich growth conditions. The characteristic spectrum observed for As-rich growth conditions does not vary significantly in samples grown in different MBE systems and with different shallow donors (Si, Sn, and Ge). Trap concentrations in different samples from different systems vary from a maximum of $1.6 \times 10^{14} \text{ cm}^{-3}$ to a minimum in the mid 10^{12} cm^{-3} range. A thirty-fold reduction in trap concentration is observed in growth systems which have been specifically designed to reduce spurious chemical contamination. This fact, coupled with a comparison of the MBE electron traps with those observed in electron-irradiated *n*-GaAs indicates that most of the observed electron traps in MBE *n*-GaAs are due to chemical contaminants. A comparison with high-quality epitaxial *n*-GaAs grown by vapor- and liquid-phase epitaxy shows that all three types of growth

(MBE, VPE, and LPE) have distinctly different electron trap spectra with the best samples from all techniques having electron trap concentrations between 0.1 and 0.7 eV from the conduction band typically in the low to mid 10^{12} cm^{-3} range.

ACKNOWLEDGMENTS

The authors wish to thank J. V. DiLorenzo, H. M. Cox, and L. C. Luther for providing the VPE *n*-GaAs, R. A. Logan and H. G. White for the LPE *n*-GaAs, and L. C. Kimerling for the 1-MeV electron-irradiated LPE *n*-GaAs. They wish to thank C. Radice and J. W. Robinson for technical assistance in growing the MBE layers and A. J. Williams for fabricating and testing the Schottky-barrier diodes used in this study.

- ¹A. Y. Cho and F. K. Reinhart, *J. Appl. Phys.* **45**, 1812 (1974).
- ²A. Y. Cho and D. R. Ch'en, *Appl. Phys. Lett.* **28**, 30 (1976).
- ³A. Y. Cho, C. N. Dunn, R. L. Kuvass, and W. E. Schroeder, *Appl. Phys. Lett.* **25**, 224 (1974).
- ⁴A. Y. Cho, W. C. Ballamy, C. N. Dunn, R. L. Kuvass, and W. E. Schroeder, *International Electron Device Meeting Technical Digest* (IEEE, New York, 1974), p. 24.8.
- ⁵S. Asai, S. Ishioka, H. Kurono, S. Takahashi, and H. Kodera, *Jpn. J. Appl. Phys. Suppl.* **42**, 71 (1973).
- ⁶A. Mircea and A. Mitonneau, *Appl. Phys.* **8**, 15 (1975).
- ⁷D. V. Lang, *J. Appl. Phys.* **45**, 3023 (1974).
- ⁸F. Hasegawa and A. Majerfeld, *Electron. Lett.* **11**, 286 (1975).
- ⁹A. Y. Cho, *J. Vac. Sci. Technol.* **8**, S31 (1971).
- ¹⁰A. Y. Cho, *J. Appl. Phys.* **42**, 2075 (1971).
- ¹¹G. L. Miller, *IEEE Trans. Electron. Devices* **ED-19**, 1103 (1972).
- ¹²D. V. Lang and R. A. Logan, *J. Electron. Mater.* **4**, 1053 (1975).
- ¹³D. V. Lang and C. H. Henry, *Phys. Rev. Lett.* **35**, 1525 (1975).
- ¹⁴A. Y. Cho and H. C. Casey, Jr., *Appl. Phys. Lett.* **25**, 288 (1974).
- ¹⁵H. C. Casey, Jr., A. Y. Cho, and P. A. Barnes, *IEEE J. Quantum Electron.* **QE-11**, 467 (1975).
- ¹⁶A. Y. Cho and I. Hayashi, *J. Appl. Phys.* **42**, 4422 (1971).
- ¹⁷A. Y. Cho and I. Hayashi, *Solid-State Electron.* **14**, 125 (1971).
- ¹⁸M. Ilegems and R. Dingle, *Proc. Int. Conf. on GaAs and Related Compounds* (Institute of Physics, London, 1975), p. 1.
- ¹⁹See references to O-peak literature in Refs. 6 and 12.
- ²⁰D. V. Lang and L. C. Kimerling, *Lattice Defects in Semiconductors*, 1974 (Inst. of Physics, London, 1975), p. 581.